

Phase equilibria in the ternary system Ce–Ti–Sn at 600°C

Oleksandr SENCHUK^{1*}, Yaroslav TOKAYCHUK¹, Pavlo DEMCHENKO¹, Roman GLADYSHEVSKII¹

¹ Department of Inorganic Chemistry, Ivan Franko National University of Lviv, Kyryla i Mefodiya St. 6, 79005 Lviv, Ukraine

* Corresponding author. Tel.: +38-032-2394506; e-mail: senchuk91@gmail.com

Received December 7, 2015; accepted December 30, 2015; available on-line September 19, 2016

The isothermal section of the phase diagram of the ternary system Ce–Ti–Sn was constructed in the whole concentration range at 600°C by means of X-ray powder diffraction. The binary compounds of the systems Ce–Sn and Ti–Sn dissolve negligible amounts of the third component. Two ternary compounds, CeTi₆Sn₄ and ~Ce₃TiSn₅, were found. The crystal structure of the compound CeTi₆Sn₄ belongs to the structure type ZrFe₆Ge₄ (Pearson symbol *hR33*, space group *R-3m*, *a* = 5.8101(11), *c* = 22.971(5) Å). It completes the row of isotypic RTi₆Sn₄ compounds with ZrFe₆Ge₄-type structure (*R* = Y, La-Nd, Sm, Gd-Tm, Lu).

Cerium / Titanium / Tin / X-ray powder diffraction / Phase diagram / Crystal structure

1. Introduction

Among the ternary systems *R*–Ti–Sn, where *R* is a rare-earth metal, the isothermal sections at 200°C have been constructed in the whole concentration regions for the systems La–Ti–Sn [1], Ce–Ti–Sn [2], and Gd–Ti–Sn [3]. The Sn-poor region (0-40 at.% Sn) of the ternary system Dy–Ti–Sn has been investigated at different temperatures (900, 1100, 1200, and 1400°C) [4-6] and the liquidus and solidus projections have been constructed [7]. No ternary compounds were found in the systems with *R* = La and Ce at 200°C, but ternary phases of composition RTi₆Sn₄ were reported in the systems with Gd [3] and Dy [8]. Isotypic ZrFe₆Ge₄-type RTi₆Sn₄ compounds have so far been found with *R* = Y, La-Nd, Sm, Gd-Tm, Lu [3,8-10]. To our knowledge, no information is available about the phase diagrams or ternary compounds of the systems *R*–{Zr,Hf}–Sn.

The binary systems that delimit the ternary system Ce–Ti–Sn have been studied in the whole concentration range and the corresponding phase diagrams constructed. Eight binary compounds were found in the system Ce–Sn [11,12]. The compounds Ce₅Sn₄, Ce₃Sn₅, and CeSn₃ melt congruently at 1515, 1180, and 1170°C, respectively, whereas Ce₃Sn, Ce₅Sn₃, Ce₁₁Sn₁₀, Ce₃Sn₇, and Ce₂Sn₅ form *via* peritectic reactions at 940, 1505, 1375, 1135, and 1145°C, respectively. A certain homogeneity range is believed to exist for Ce₁₁Sn₁₀. An additional compound, Ce₂Sn₃, was reported later [13]. The existence of five binary compounds has been

established in the system Ti–Sn [14,15]. The compounds Ti₃Sn and Ti₆Sn₅ melt congruently at 1670 and 1490°C, respectively, whereas Ti₂Sn, Ti₅Sn₃, and Ti₂Sn₃ form *via* peritectic reactions at 1550, ~1520, and ~750°C, respectively. Three compounds, Ti₅Sn₃, Ti₆Sn₅, and Ti₂Sn₃, are characterized by constant compositions, while for the compounds Ti₃Sn and Ti₂Sn homogeneity ranges of 1 at.% (Ti₃Sn) and 1.5 at.% (Ti₂Sn) at 600°C, respectively, were established. No binary compounds form in the system Ce–Ti.

In this work we present the results of an investigation of the phase equilibria in the system Ce–Ti–Sn at 600°C and the crystal structure of the ternary compound CeTi₆Sn₄.

2. Experimental

The investigation was carried out on 34 alloys, which were synthesized from high-purity metals (Ce ≥ 99.9 mass%, Ti ≥ 99.99 mass%, Sn ≥ 99.99 mass%) by arc melting under argon atmosphere using a water-cooled copper hearth and a tungsten electrode. Argon was additionally purified during the synthesis by a molten Ti getter. To ensure homogeneity the samples were melted twice. After synthesis the alloys were annealed at 600°C in quartz ampoules under vacuum for 1.5 month. Finally the ampoules with the samples were rapidly quenched into cold water. The weigh losses, which were controlled at all stages of the synthesis, did not exceed

2 mass% of the total mass, which was approximately 1 g for each alloy.

Phase analysis was carried out using X-ray powder diffraction data collected at room temperature on a diffractometer DRON-2.0M (Fe $K\alpha$ radiation, $\lambda = 1.93801$ Å, angular range $30^\circ \leq 2\theta \leq 90^\circ$, step 0.05°). It was performed by comparison of the experimental patterns with theoretical patterns of the metals and known binary compounds [16], using the program PowderCell [17]. The cell parameters of the individual phases were refined with the UnitCell program [18]. The structure of the ternary compound $CeTi_6Sn_4$ was refined on X-ray diffraction data collected on a powder diffractometer STOE Stadi P (Cu $K\alpha_1$ radiation, $\lambda = 1.54056$ Å, linear detector, $6^\circ \leq 2\theta \leq 110^\circ$, step 0.015°). The profile and structural parameters were refined by the Rietveld method using the FullProf Suite program package [19].

3. Results and discussion

3.1. The binary systems

The existence of 14 compounds in the boundary binary systems Ce–Sn and Ti–Sn at 600°C was confirmed: Ce_3Sn , Ce_5Sn_3 , Ce_5Sn_4 , $Ce_{11}Sn_{10}$, Ce_2Sn_3 , Ce_3Sn_5 , Ce_3Sn_7 , Ce_2Sn_5 , $CeSn_3$, Ti_3Sn , Ti_2Sn , Ti_5Sn_3 , Ti_6Sn_5 , and Ti_2Sn_3 . Crystallographic data, including cell parameters refined from X-ray powder diffraction data obtained for different alloys, are summarized in Table 1.

3.2. Isothermal section of the phase diagram of the system Ce–Ti–Sn at 600°C

The isothermal section of the phase diagram of the ternary system Ce–Ti–Sn at 600°C is shown in Fig. 1. It contains 19 single-phase, 37 two-phase and 19

three-phase fields. The highest numbers of equilibria (7) are formed with the phases Ti_6Sn_5 and $CeTi_6Sn_4$. The limits of the liquid part at the tin corner was extrapolated from its limits at 600°C in the binary systems: 6.7 at.% in the system Ce–Sn and 4.1 at.% in the system Ti–Sn [11,15]. The binary compounds of the systems Ce–Sn and Ti–Sn do not dissolve noticeable amounts of the third component. Two ternary compounds of constant compositions $CeTi_6Sn_4$ and $\sim Ce_3TiSn_5$ were found at 600°C. The exact composition of the latter was not established, therefore, the equilibria involving this phase are drawn by dotted lines in Fig. 1.

The phase diagram of the Ce–Ti–Sn system is similar to the phase diagrams reported for other R –Ti–Sn systems ($R = La, Gd, Dy$) [1,3-5,7,8]. These systems are all characterized by negligible solubility of the third component in the binary compounds and a low number of ternary compounds. Ternary compounds RTi_6Sn_4 with $ZrFe_6Ge_4$ -type structure have been found in the systems with $R = Y, La-Nd, Sm, Gd-Tm, Lu$ [3,8-10,20]. Comparing the isothermal section of the ternary system Ce–Ti–Sn at 600°C investigated here, with the section at 200°C determined earlier [2], one may note the increased complexity of the interactions between the components at the higher temperature, underlined by the formation of two ternary compounds, absent at 200°C.

3.3. The ternary compound $CeTi_6Sn_4$

The crystal structure of the ternary compound $CeTi_6Sn_4$ was determined by means of X-ray powder diffraction. It was refined by the Rietveld method, starting from the atom coordinates of the structure type $ZrFe_6Ge_4$ (Pearson symbol $hR33$, space group $R-3m$) [21]. The sample used for the refinement contained four phases. Only the scale factors and cell

Table 1 Crystallographic data for the binary compounds of the systems Ce–Sn and Ti–Sn.

Compound	Sample composition	Structure type, Pearson symbol, space group	Cell parameters, Å		
			<i>a</i>	<i>b</i>	<i>c</i>
Ce_3Sn	$Ce_{60}Ti_{20}Sn_{20}$	$Cu_3Au, cP4, Pm-3m$	4.91342(17)	-	-
Ce_5Sn_3	$Ce_{55.5}Ti_{11}Sn_{33.5}$	$W_5Si_3, tI32, I4/mcm$	12.6067(3)	-	6.2394(3)
Ce_5Sn_4	$Ce_{52.5}Ti_5Sn_{42.5}$	$Sm_5Ge_4, oP36, Pnma$	8.3339(8)	16.0284(11)	8.4837(5)
$Ce_{11}Sn_{10}$	$Ce_{52.4}Sn_{47.6}$	$Ho_{11}Ge_{10}, tI84, I4/mmm$	11.9952(6)	-	17.7948(17)
Ce_2Sn_3	$Ce_{40}Sn_{60}$	$Nd_2Sn_3, aP20, P-1^a$	6.4251(3)	8.5215(8)	11.1958(5)
Ce_3Sn_5	$Ce_{30}Ti_5Sn_{65}$	$Pu_3Pd_5, oS32, Cmc$	10.2446(10)	8.2009(16)	10.6484(11)
Ce_3Sn_7	$Ce_{25}Ti_{10}Sn_{65}$	$Ce_3Sn_7, oS20, Cmmm$	4.5568(3)	25.7938(14)	4.6343(5)
Ce_2Sn_5	$Ce_{25}Ti_5Sn_{70}$	$Ce_2Sn_5, oS28, Cmmm$	4.5955(3)	35.214(3)	4.6420(4)
$CeSn_3$	$Ce_{25}Ti_5Sn_{70}$	$Cu_3Au, cP4, Pm-3m$	4.7229(3)	-	-
Ti_3Sn	$Ce_9Ti_{55}Sn_{36}$	$Mg_3Cd, hP8, P6_3/mmc$	5.9103(12)	-	4.7678(11)
Ti_2Sn	$Ce_9Ti_{55}Sn_{36}$	$Ni_2In, hP6, P6_3/mmc$	4.6450(10)	-	5.6724(16)
Ti_5Sn_3	$Ce_5Ti_{57.5}Sn_{37.5}$	$Mn_5Si_3, hP16, P6_3/mcm$	8.0603(4)	-	5.4591(5)
Ti_6Sn_5	$Ti_{40}Sn_{60}$	$Ti_6Sn_5, hP22, P6_3/mmc$	9.2347(3)	-	5.7042(3)
Ti_2Sn_3	$Ti_{40}Sn_{60}$	$Ti_2Sn_3, oS40, Cmce$	5.9543(6)	19.9506(19)	7.0203(7)

^a $\alpha = 107.446(5)$, $\beta = 96.730(4)$, $\gamma = 99.678(4)^\circ$.

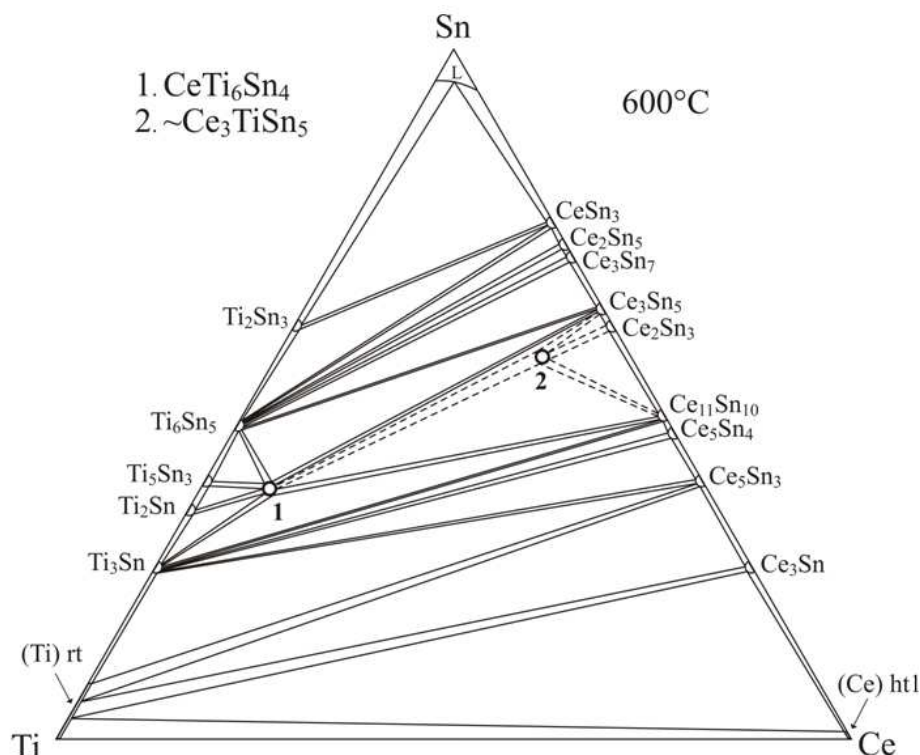


Fig. 1 Isothermal section of the phase diagram of the system Ce–Ti–Sn at 600°C.

parameters were refined for the admixture phases, and the profile parameters were constrained to be equal to those of the main phase. At the final step, in total 24 parameters were allowed to vary: 2θ shift (with $\sin(2\theta)$ dependence sample transparency coefficient), four scale factors, eight cell parameters, six profile parameters (pseudo-Voigt profile), four positional parameters, and one texture parameter. The isotropic displacement parameters were constrained as follows: $B_{\text{iso}}(\text{Ce}) = 0.5$, $B_{\text{iso}}(\text{Ti}) = 1.0$, $B_{\text{iso}}(\text{Sn}) = 0.7 \text{ \AA}^2$, and were not refined. The background was defined by linear interpolation between 43 points. Experimental and calculated X-ray powder diffraction patterns and the difference between them, for the sample of nominal composition $\text{Ce}_9\text{Ti}_{55}\text{Sn}_{36}$ are shown in Fig. 2. Experimental details and crystallographic data for the individual phases are listed in Table 2. Atomic coordinates in the structure of the ternary compound CeTi_6Sn_4 are listed in Table 3, while the interatomic distances, coordination numbers and coordination polyhedra are presented in Table 4.

The ternary compound CeTi_6Sn_4 crystallizes in the rhombohedral structure type ZrFe_6Ge_4 (Pearson symbol $hR33$, space group $R\bar{3}m$, $a = 5.8101(11)$, $c = 22.971(5) \text{ \AA}$). The structure is characterized by an ordered distribution of atoms in four sites: the site in Wyckoff position $3a$ is occupied by Ce atoms, the two sites in $6c$ by Sn atoms and the site in $18h$ by Ti atoms. The Ce atoms center 20-vertex polyhedra $\text{CeTi}_{12}\text{Sn}_8$ (hexagonal prisms Ti_{12} with eight additional Sn atoms above the faces). The coordination

polyhedra of the Sn atoms are anticuboctahedra $\text{Sn}_1\text{Ce}_3\text{Ti}_6\text{Sn}_3$ and truncated hexagonal bipyramids Sn_2CeTi_9 . The Ti atoms are surrounded by 11-vertex pseudo Frank-Kasper polyhedra TiTi_6Sn_5 , which can be described as distorted defect cuboctahedra. The structure can be seen as a stacking of layers of slightly distorted $\text{Ce}_3\text{Ti}_6\text{Sn}_3$ anticuboctahedra and layers of truncated CeTi_9 hexagonal bipyramids along the crystallographic direction $[001]$. The titanium atoms form kagome nets perpendicular to $[001]$.

CeTi_6Sn_4 can be added to the row of already known isotypic compounds $R\text{Ti}_6\text{Sn}_4$ with ZrFe_6Ge_4 -type structure. It maybe noted that this structure type is sometimes referred to as LiFe_6Ge_4 , since the structure of this compound, which was refined in space group $C2/m$ [22], can be described in space group $R\bar{3}m$ after minor adjustments [23]. At present, $R\text{Ti}_6\text{Sn}_4$ compounds with ZrFe_6Ge_4 -type structure are known for $R = \text{Y}$, La–Nd, Sm, Gd–Tm, and Lu [3,8–10], *i.e.* for both light and heavy rare-earth metals, Eu and Yb being not included in the list. During the refinement of the structures of the ternary phases with $R = \text{Tm}$ and Lu on X-ray single-crystal data [9], the site in Wyckoff position $3a$ was found to be occupied by a statistical mixture of R and Sn atoms, leading to the off-stoichiometric compositions $\text{Tm}_{0.86(1)}\text{Ti}_6\text{Sn}_{4.14(1)}$ and $\text{Lu}_{0.92(1)}\text{Ti}_6\text{Sn}_{4.08(1)}$, respectively. This indicates that small homogeneity ranges probably exist. The chemical bonding in LuTi_6Sn_4 and a series of isotypic germanides was studied based on DFT calculations in [20].

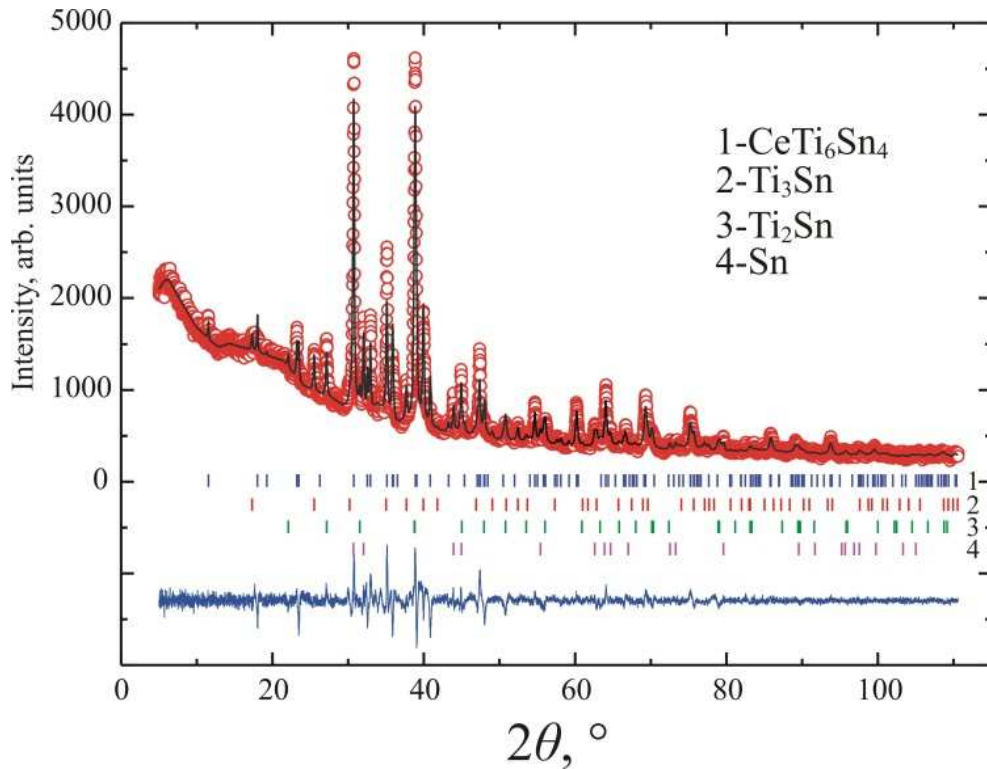


Fig. 2 Experimental (circles), calculated (solid line) and difference (bottom) X-ray powder diffraction patterns of the sample $\text{Ce}_9\text{Ti}_{55}\text{Sn}_{36}$. Vertical bars indicate the positions of the reflections of the individual phases.

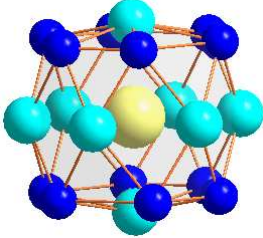
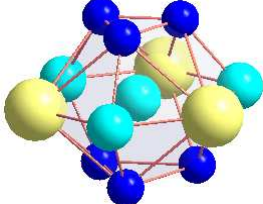
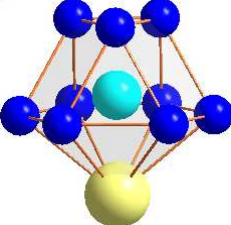
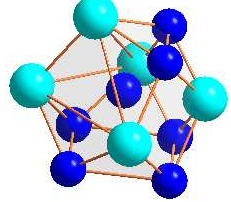
Table 2 Experimental details and crystallographic data for the individual phases in the sample $\text{Ce}_9\text{Ti}_{55}\text{Sn}_{36}$.

Compound	CeTi_6Sn_4	Ti_3Sn	Ti_2Sn	Sn
Content, mass%	53.3(12)	19.0(4)	16.6(4)	11.1(2)
Structure type	ZrFe_6Ge_4	Mg_3Cd	Ni_2In	Sn
Pearson symbol	$hR33$	$hP8$	$hP6$	$tI4$
Space group	$R\text{-}3m$ (#166)	$P6_3/mmc$ (#194)	$P6_3/mmc$ (#194)	$I4_1/amd$ (#141)
Cell parameters:				
a , Å	5.8101(11)	5.9103(12)	4.6450(10)	5.8254(12)
c , Å	22.971(5)	4.7678(11)	5.6724(16)	3.1801(7)
Cell volume V , Å ³	671.5(2)	144.23(5)	105.99(5)	107.92(4)
Formula units per unit cell Z	3	2	2	4
Density D_x , g/cm ³	6.692	6.040	6.719	7.305
Preferred orientation: value [direction]	0.973(9) [001]	-	-	-
FWHM parameters:				
U			0.45(5)	
V			-0.16(4)	
W			0.041(6)	
Shape parameter η			0.97(2)	
Asymmetry parameters			0.026(9), 0.007(2)	
Number of reflections	155	57	43	26
Reliability factors:				
R_B	0.0737	0.106	0.0835	0.0463
R_F	0.0446	0.0653	0.0484	0.0350
R_p			0.0462	
R_{wp}			0.0637	
χ^2			2.88	

Table 3 Atomic coordinates in the structure of CeTi₆Sn₄ (ZrFe₆Ge₄, *hR33*, *R-3m*, *a* = 5.8101(11), *c* = 22.971(5) Å)

Site	Wyckoff position	<i>x</i>	<i>y</i>	<i>z</i>	<i>B</i> _{iso} , Å ²
Ce	3 <i>a</i>	0	0	0	0.5
Sn1	6 <i>c</i>	0	0	0.3340(3)	0.7
Sn2	6 <i>c</i>	0	0	0.1329(3)	0.7
Ti	18 <i>h</i>	0.5006(14)	0.4994(14)	0.1034(5)	1.0

Table 4 Interatomic distances (δ), coordination numbers (CN) and coordination polyhedra in the structure of CeTi₆Sn₄ (ZrFe₆Ge₄, *hR33*, *R-3m*, *a* = 5.8101(11), *c* = 22.971(5) Å).

Atoms		δ , Å	CN	Polyhedron
Ce	- 2 Sn2 - 6 Sn1 - 12 Ti	3.053(7) 3.3545(6) 3.752(9)	20	 CeTi ₁₂ Sn ₈
Sn1	- 2 Ti - 4 Ti - 3 Sn1 - 3 Ce	2.899(11) 2.917(11) 3.3545(6) 3.3545(6)	12	 Sn1Ce ₃ Ti ₆ Sn ₃
Sn2	- 3 Ti - 6 Ti - 1 Ce	2.786(10) 2.983(9) 3.053(7)	10	 Sn2CeTi ₉
Ti	- 1 Sn2 - 2 Ti - 1 Sn1 - 2 Ti - 1 Sn1 - 2 Sn2 - 2 Ti	2.786(10) 2.895(12) 2.899(11) 2.916(12) 2.917(11) 2.983(9) 3.359(12)	11	 TiTi ₆ Sn ₅

4. Conclusions

The ternary system Ce–Ti–Sn at 600°C is characterized by the existence of two ternary compounds with constant compositions CeTi₆Sn₄ and ~Ce₃TiSn₅. The binary compounds of the systems Ce–Sn and Ti–Sn do not dissolve noticeable amounts of the third component. The ternary compound CeTi₆Sn₄ crystallizes in the structure type ZrFe₆Ge₄

and is characterized by an ordered distribution of the atoms.

Acknowledgement

This work was carried out under the grant of the Ministry of Education and Science of Ukraine No. 0115U003257.

References

- [1] Y. Zhan, Y. Xu, H. Xie, Z. Yu, Y. Wang, Y. Zhuang, *J. Alloys Compd.* 459 (2008) 174-176.
- [2] J. Hu, Y. Zhan, J. She, X. Zhang, *J. Alloys Compd.* 496 (2010) 155-158.
- [3] J. Ma, Y. Zhan, J. She, Z. Yang, J. Liang, *J. Alloys Compd.* 489 (2010) 384-388.
- [4] Yu.V. Fartushna, A.V. Kotko, M.V. Bulanova, *Chem. Met. Alloys 2* (2009) 83-88.
- [5] M. Bulanova, Yu. Fartushna, K. Meleshevich, A. Samelyuk, *J. Alloys Compd.* 578 (2013) 261-266.
- [6] M. Bulanova, Yu. Podrezov, Yu. Fartushna, *Intermetallics* 14 (2006) 435-443.
- [7] Y. Fartushna, K. Meleshevich, A. Samelyuk, M. Bulanova, *Int. J. Mater. Res.* 101 (2010) 1298-1310.
- [8] Yu. Fartushna, J. Stępeń-Damm, L.G. Aksel'rud, M.B. Manyako, B.D. Belan, M.V. Bulanova, R.E. Gladyshevskii, *Coll. Abstr. XI Int. Conf. Cryst. Chem. Intermet. Compd.*, Lviv, 2010, p. 66.
- [9] M. Eul, T. Langer, R. Pöttgen, *Intermetallics* 20 (2012) 98-103.
- [10] O. Senchuk, Ya. Tokaychuk, P. Demchenko, R. Gladyshevskii, *Coll. Abstr. XX Int. Sem. Phys. Chem. Solids*, Lviv, 2015, p. 37.
- [11] T.B. Massalski, H. Okamoto, P.R. Subramanian (Eds.), *Binary Alloy Phase Diagrams*, 2nd edition, ASM International, Materials Park (OH), 1990, p.1112-1115.
- [12] P. Riani, D. Mazzone, G. Zanocchi, R. Marazza, R. Ferro, *J. Phase Equilib.* 19 (1998) 239-251.
- [13] M.L. Fornasini, P. Manfrinetti, A. Palenzona, S.K. Dhar, *Z. Naturforsch. B* 58 (2003) 521-527.
- [14] C. Kuper, W. Peng, A. Pisch, F. Goesmann, R. Schmid-Fetzer, *Z. Metallkde.* 89 (1998) 855-862.
- [15] H. Okamoto, *J. Phase Equilib. Diffus.* 31 (2010) 202-203.
- [16] P. Villars, K. Cenzual (Eds.), *Pearson's Crystal Data. Crystal Structure Database for Inorganic Compounds*, Release 2014/15, ASM International, Materials Park (OH), 2014.
- [17] W. Kraus, G. Nolze, Powder Cell for Windows (version 2.4), Federal Institute for Materials Research and Testing, Berlin, 1999.
- [18] T. Holland, S. Redfern, *Mineral. Mag.* 61 (1997) 65-77.
- [19] J. Rodríguez-Carvajal, *Commission on Powder Diffraction (IUCr) Newsletter.* 26 (2001) 12-19.
- [20] S.F. Matar, T. Fickenscher, B. Gerke, O. Niehaus, U.Ch. Rodewald, A.F. Al Alam, N. Ouaini, R. Pöttgen, *Solid State Sci.* 39 (2015) 82-91.
- [21] R.R. Olenych, O.I. Bodak, *Tez. Dokl. VI Sov. Kristallokhim. Neorg. Koord. Soed.*, Lviv, 1992, p. 204.
- [22] E. Welk, H.U. Schuster, *Z. Naturforsch. B* 32 (1977) 749-752.
- [23] K. Cenzual, L.M. Gelato, M. Penzo, E. Parthé, *Z. Kristallogr.* 193 (1990) 217-242.